Materials Science and Engineering C 61 (2016) 23–31

Contents lists available at ScienceDirect

Materials Science and Engineering C

journal homepage: www.elsevier.com/locate/msec

Effects of polar solvents on the mechanical behavior of fish scales

Sandra Murcia [a], Guihua Li [b], Mobin Yahyazadehfar [a], Mikaela Sasser [c], Alex Ossa [d], D. Arola [a,*]

[a] Department of Materials Science and Engineering, University of Washington, Seattle, WA, USA
[b] School of Electrical Engineering and Automation, Anhui University, Hefei, China
[c] Department of Mechanical Engineering, University of Maryland Baltimore County, Baltimore, MD, USA
[d] School of Engineering, Universidad Eafit, Medellín, Colombia

ARTICLE INFO

Article history:
Received 9 June 2015
Received in revised form 10 November 2015
Accepted 3 December 2015
Available online 10 December 2015

Keywords:
Cyprinus carpio
Fish scales
Fracture resistance
Mechanical behavior
Polar solvents

ABSTRACT

Fish scales are unique structural materials that serve as a form of natural armor. In this investigation the mechanical behavior of scales from the *Cyprinus carpio* was evaluated after exposure to a polar solvent. Uniaxial tensile and tear tests were conducted on specimens prepared from the scales of multiple fish extracted from near the head, middle and tail regions, and after exposure to ethanol for periods from 0 to 24 h. Submersion in ethanol caused instantaneous changes in the tensile properties regardless of anatomical site, with increases in the elastic modulus, strength and modulus of toughness exceeding 100%. The largest increase in properties overall occurred in the elastic modulus of scales from the tail region and exceeded 200%. Although ethanol treatment had significant effect on the tensile properties, it had limited influence on the tear resistance. The contribution of ethanol to the mechanical behavior appears to be derived from an increase in the degree of interpeptide hydrogen-bonding of the collagen molecules. Spatial variations in the effects of ethanol exposure on the mechanical behavior arise from the differences in degree of mineralization and lower mineral content in scales of the tail region.

1. Introduction

Over the last decade there has been substantial effort placed on understanding the microstructure and mechanical behavior of selected structural materials in nature. The natural armors of the alligator, armadillo, fish, pangolin and others are excellent examples of materials in this category [1–9]. These materials have evolved to provide protection from outstanding threats without encumbering locomotion. While the "armor" of the aforementioned group of animals may appear disparate, they share the quality of most composite materials, i.e. they are constructed of a combination of constituents and possess mechanical properties superior to those of the individual components.

Elasmoid scales are found on teleost fish and have an interesting structure. In comparison to the bony or ganoid scales, elasmoid scales are relatively thin and compliant, which endow ease of movement to the fish. A number of studies have been conducted on elasmoid scales including those of the Carp (*Cyprinus carpio*) [6,7], Striped Bass (*Morone saxatilis*) [8,10,11], *Pagrus major* [12], and *Arapaima gigas* [1–3,13–15]. The structure of elasmoid scales is hierarchical and is composed of two primary layers (Fig. 1). The external or "limiting layer" is highly mineralized and consists of calcium-deficient apatite or calcium carbonate, depending on the fish [6,13,16]. The internal layer or "elasmodine" is a composite of type I collagen fibers and apatite mineral. The fibers are sparsely reinforced with mineral and organized in discrete plies, which are arranged in the form of a plywood structure. The diameter of the collagen fibers is near 1 μm, and they are constructed of an assembly of fibrils roughly 100 nm in diameter [2,6,10,11,16,17]. The individual fibrils and interfibrillar minerals of scales have been observed in evaluations performed with transmission electron microscopy and atomic force microscopy [1,6,16].

Elasmoid scales exhibit a strong mineral gradient across the thickness, which is reflected in the mechanical properties. There is a substantial reduction in the hardness and elastic modulus distributions from the exterior to the interior layers [4,13]. This gradient in properties plays an important role on the puncture resistance [11]. The limiting layer (LL) acts as initial barrier that dissipates energy by brittle fracture. The fracture propagates to the interface with the external elasmodine (EE), resulting in delamination. Once the LL and EE have undergone gross failure, further penetration is resisted by the internal elasmodine and a concert of mechanisms that are largely dependent on the collagen fibrils. Delamination between adjacent plies and fibrils is key to the fracture resistance of scales and bestows them with incredible notch insensitivity [10].

Due to the rather large organic content, the mechanical behavior of fish scales has been found to be sensitive to hydration. Ikoma et al. [12] evaluated the tensile properties of dehydrated scales of *P. major* and reported an elastic modulus and tensile strength of 2.2 ± 0.3 GPa and 93 ± 1.8 MPa, respectively. Scales of *A. gigas* exhibited an elastic modulus of 0.8 ± 0.1 GPa and tensile strength of 22.3 ± 3.9 MPa in the hydrated condition, which increased to 1.4 ± 0.2 GPa and 53.9 ±

* Corresponding author at: Department of Materials Science and Engineering, University of Washington, Roberts Hall, Box 352120, Seattle, WA 98195, USA.
E-mail address: darola@uw.edu (D. Arola).

http://dx.doi.org/10.1016/j.msec.2015.12.007
0928-4931/

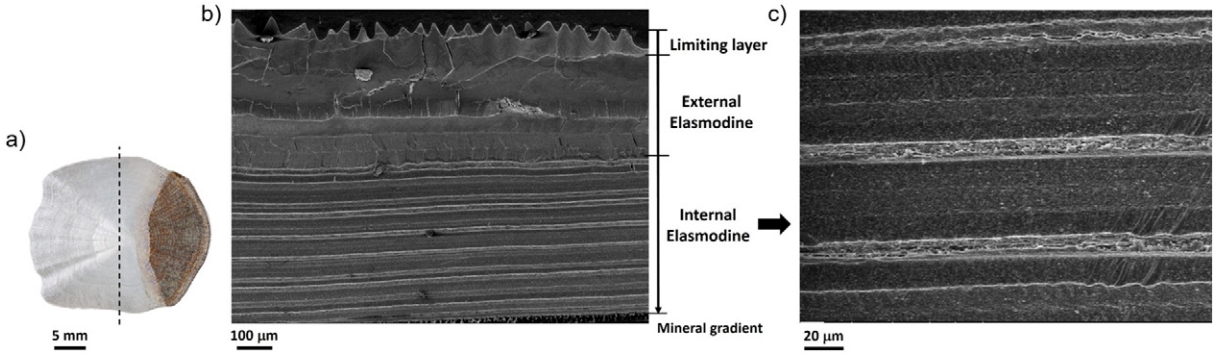

Fig. 1. Hierarchical structure of scales from the *Cyprinus carpio*. a) Individual scale with section line indicating the location of cross-section shown in (b) and (c). b) Highly magnified view of the scale structure across the thickness. Evident are the limiting layer at the surface of the scale, the external elasmodine and the internal elasmodine, which is located closest to the body of the fish. c) Ply distribution from a portion of the internal elasmodine.

8.4 MPa, respectively with dehydration [13]. Garrano et al. [6] found that the relative importance of hydration to the mechanical behavior of carp scales is a function of anatomical position. Scales from the tail underwent the greatest changes in performance with dehydration. One limitation of these previous evaluations is that dehydration was achieved by simple free convection in air. That process results in removal of the free water molecules, but requires substantial time and does not remove bound water [18–20]. Air-drying of *A. gigas* scales resulted in a residual water content of 16% in comparison to 30% for the hydrated scale [13].

Changes in the mechanical behavior with dehydration of collagen-based structural materials are at least partially related to the increase in interpeptide bonding with removal of the water molecules [18,19]. Dehydration of collagenous materials can be achieved by immersion in polar solvents, which displaces the water molecules residing within the collagen matrix with solvent and promotes hydrogen bonding between the peptide chains. Dehydration in this manner avoids other concerns related to dehydration in air. Therefore, the primary objective of this study was to evaluate the changes in mechanical behavior of teleost scales with exposure to polar solvents. A combination of uniaxial tension and tear tests was used to evaluate the changes in constitutive behavior and the resistance to fracture.

2. Materials and methods

Scales of the *C. carpio* (i.e. the common freshwater carp) were obtained by extraction from across the body of seven different fish after the methods of Garrano et al. [6]. These fish were marketed as East Asian carp, and no additional information was available for record. The scales were obtained nearly equidistant between the ventral and dorsal aspects of the body and from three regions including adjacent to the head, mid-length (beneath the dorsal fin) and near the tail (Fig. 2a). All of the scales were less than 1 mm thick and possessed a diameter that depended on the anatomical position. Scales from the head region had an effective diameter (d) ≥25 mm. Those obtained from the middle and tail regions ranged between 22 ≤ d ≤ 25 mm and

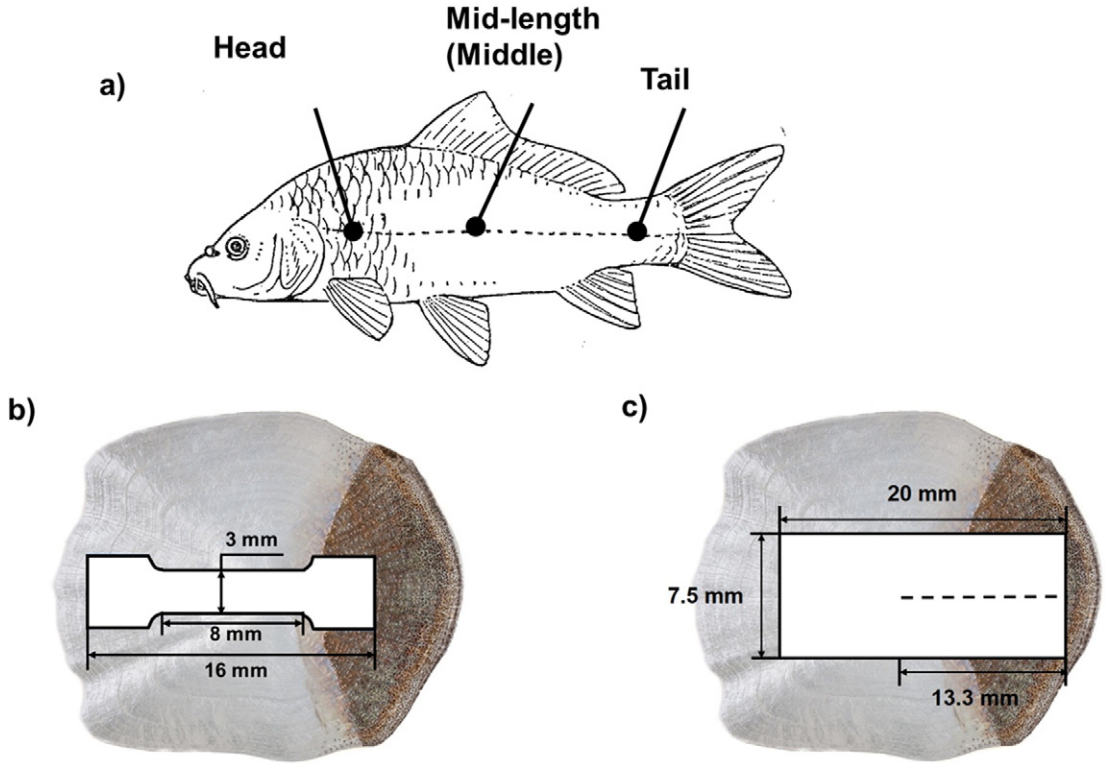

Fig. 2. Details regarding the specimens prepared for characterizing mechanical behavior. (a) Anatomical position of the extracted scales [6], (b) extracted scale with location and geometry of the stamped tensile specimens, and (c) geometry of the tear specimens.

19 ≤ d ≤ 22 mm, respectively. After extraction, the scales were stored in Hanks Balanced Salt Solution (HBSS) at room temperature and evaluated within two weeks of harvesting the fish.

Conventional dog-bone shaped tensile samples were sectioned from the scales using a punch and stamping process [21]. All of the specimens were obtained with alignment parallel to the fish length, in recognition that the scales may exhibit anisotropy [1,7,11]. The specimens possessed a gage section length and width of 8 mm and 3 mm, respectively (Fig. 2b). In recognition of potential variations in thickness of the scales [22], a single sample was stamped from the center region of each scale where the thickness is most uniform. The gage section was then measured to assess the change in thickness over the length. Overall, the thickness of the samples changed less than 50 μm over the gage section length; the lowest thickness was used in estimating the stress. After sectioning, the specimens were returned to the HBSS bath at room temperature.

Tensile testing was performed with the fish scale specimens submerged in a liquid bath at room temperature. The loading was performed under displacement control using a dedicated universal testing machine complemented with a microscopic imaging system. The system has a full-scale load range of 50 N and load precision of 0.1%. A stroke rate of 0.2 mm/min was utilized, which corresponded to a strain rate of roughly $5 \times 10^{-4}\ s^{-1}$ according to the specimen gage length. All specimens were tested to first ply failure/fracture following Garrano et al. [6]. Tension tests were performed after time-controlled storage of the scale in an ethanol bath at room temperature for periods of t = 0, 2, 4, 8 and 24 h. The exposure period for the t = 0 h condition consisted of approximately 5 min exposure. Additional tests were performed on hydrated scales tested in HBSS, which served as the control. Five specimens were prepared from each anatomical region (head, middle and tail) and for every hydration condition, which resulted in a total of approximately 90 specimens prepared and evaluated from each fish.

The axial strains that developed within the specimen gage section were obtained using Digital Image Correlation (DIC). Details regarding DIC and applications to hard tissues and microscopic DIC can be found in [21,23,24]. The outer surface of the scales is largely mineral (of the limiting layer), rendering it brittle in comparison to the internal elasmodine. Thus, the interior surface of the scale specimens was monitored during the tensile tests as described in [6]. The optical system consisted of a F32 5.6-11 C-mount objective lens, a 5 mm extension tube and a CV-A1 CCD camera (JAI America Inc) with a coherent and uniform illumination system. Sequential images were acquired incrementally during each tensile test at a frequency of 0.1 Hz, which were synchronized with the load and displacement signal by computer control. The images were obtained with a spatial resolution of 1376 × 1035 pixels and 256 gray scales. The images encompassed an area of approximately 5.6 × 4.2 mm and were processed using sub-pixel resolution, which provided a displacement resolution of approximately 4 μm.

Mechanical properties of the scales were determined from results of the tension tests of each hydration condition using the engineering stress–strain definitions. The elastic modulus (E), strength (S) and modulus of toughness (MOT) were determined for each specimen. The elastic modulus was determined using the tangent method for strains less than 1% and the strength was defined by the maximum stress realized by the sample. The modulus of toughness was calculated by integrating the area under the stress–strain curves as a function of strain until first ply failure. Ply failure was identified by a sharp reduction in the axial load.

The influence of polar solvents on the mechanical behavior was also evaluated in terms of the resistance to fracture under Mode III shear. Trouser-shaped tear specimens were sectioned from the scales using a specially designed punch and stamp as previously described [7]. Similar to the tensile specimens, the samples were stamped with respect to the longitudinal axis to minimize potential effects of anisotropy (Fig. 2c). Each sample was obtained from the center of the scale, such that crack extension occurred within the region of uniform thickness. After sectioning, the specimens were placed in a bath of HBSS or ethanol at room temperature.

Tear testing was performed under displacement control loading using a universal testing machine (Instron ElectroPuls E1000). The instrument's load cell has a full-scale range of 250 N and precision of 0.01%. To minimize elongation of the specimen outside the region of tear, 80–90% of the legs were clamped within the compression grips during the experiments. The testing was performed using a stroke rate of 100 mm/min until complete failure of the sample after previously established methods [7]. Tear testing was conducted with the samples immersed in a bath of HBSS or ethanol at room temperature. Results of the tensile tests in ethanol revealed that after immediate exposure, further changes with additional treatment time (up to 24 h) were negligible. Therefore, tear testing was performed directly after submersion (corresponding to t = 0 h) and consisted of approximately 5 min exposure total. Consequently, eight samples were prepared from each anatomical position and for each hydration condition, resulting in an evaluation of 48 specimens taken from among the seven fish.

The energy required to tear the fish scales was estimated from the force-displacement curves of each specimen according to T = 2P/t, where P and t are the tearing force and specimen thickness, respectively [7,25]. The maximum force was identified from the tear history. The work to fracture was also quantified by integrating the area under the force-displacement curves as a function of the tear displacement. Changes in mechanical properties as a function of position of the fish body and period of ethanol exposure were evaluated for statistical significance using a Two-Way Analysis of Variance (ANOVA) and Tukeys HSD test at $\alpha = 0.05$.

The microstructure of scales within each region of evaluation was examined using optical microscopy (Olympus BX51, Tokyo, Japan) and scanning electron microscopy (JEOL, model JSM- 6010PLUS/LA, Peabody, MA). Samples from each of the three regions were sectioned in the transverse plane near the center of the scale. The sectioned scales were fixed in resin and polished with SiC abrasive paper from mesh numbers of 800 to 4000. Final polishing was performed with a diamond liquid suspension of 3 μm, followed by a liquid suspension of 1 μm Al_2O_3. The microstructure was observed over a range of magnification to distinguish important features. Those samples evaluated using the SEM were sputtered with platinum and observed in secondary electron imaging mode. In addition, an elemental analysis was conducted across the scale thickness using Energy Dispersive X-ray Spectroscopy (EDS) to quantify the chemical composition and the distribution of mineral content as a function of anatomical position. Nine discrete measurement locations were selected across the scale thickness, including one point in the limiting layer and the remaining points distributed across the elasmodine in increments of roughly 0.1 mm over the entire normalized thickness.

3. Results

Results of tensile tests performed on scales from the head region are shown in Fig. 3. The responses in this figure span the range of ethanol storage times and include those obtained for the hydrated condition. As evident from the relative distribution of curves before and after treatment, exposure to ethanol caused an immediate and substantial increase in the stiffness and strength of the scales. The changes continued with increasing duration of ethanol exposure, but they became negligible after approximately 8 h of ethanol treatment.

The stress–strain curves obtained from the specimen of each scale were used in estimating the elastic modulus, strength and modulus of toughness. Fig. 4 presents cumulative results for the mechanical properties in the three regions of evaluation as a function of ethanol exposure up to 8 h of exposure. Specifically, Fig. 4a shows the importance of

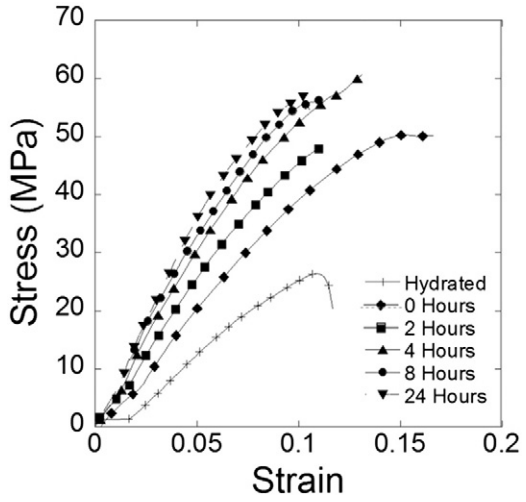

Fig. 3. Representative stress–strain curves resulting from tensile tests performed on the scale specimens after ethanol treatment for periods of 0 to 24 h. Failure was defined by first ply fracture. Results for the hydrated condition (in HBSS) are shown for comparison. The responses in this figure were obtained from scales of the head region.

ethanol treatment and period of storage on the elastic modulus. There was a significant increase ($p \le 0.05$) in the elastic modulus after immediate exposure to ethanol in all three regions evaluated. The largest change occurred in scales of the tail region, with an average increase of up to 150%. Prolonged exposure to ethanol did not cause further significant changes in the elastic modulus ($p > 0.05$). Results for the strength and the modulus of toughness are shown in Fig. 4b and c, respectively. There was a significant increase ($p \le 0.05$) in both properties with immediate exposure to the ethanol. Further increases were realized for approximately two hours of exposure. However, after two hours ($t > 2$ h) there was no further increase in the strength or MOT ($p > 0.05$).

Although both the strength and MOT exhibited similar responses after ethanol exposure, there were differences with respect to the anatomical position. The strength of scales from the middle and the tail were not significantly different from each other ($p > 0.05$), but they were significantly lower than that of the head scales ($p < 0.05$). For the MOT (Fig. 4c), results for scales from the head, middle region and tail were significantly different from each other ($p < 0.05$). It is important to note that the increase in stiffness and strength was not accompanied by a decrease in strain to failure. Rather, there was a significant increase ($p < 0.05$) in the strain at fracture after exposure to ethanol in comparison to the fully hydrated scales (not shown).

The effect of ethanol exposure on the fracture resistance of the scales was evaluated in terms of the tear energy. The energy required for fracture is shown for selected specimens from scales of the head, middle and tail regions in Fig. 5a through c, respectively. The responses presented in these figures include those obtained after immediate exposure to ethanol, and for the hydrated condition (i.e. in HBSS) as well. As evident from the tear responses, the fracture process was stable in both conditions of hydration and in all three regions of evaluation. In addition, the responses for the hydrated and dehydrated conditions appear to be similar.

A summary of results for the fracture resistance is shown in Fig. 6. Specifically, Fig. 6a shows the cumulative results for the tear energy as a function of hydration in the three regions of evaluation. Analogous results for the tear work are shown in Fig. 6b. Note that results obtained for the scales subjected to ethanol treatment corresponded to a storage period of $t = 0$ h (immediate response). Clearly the influence of ethanol

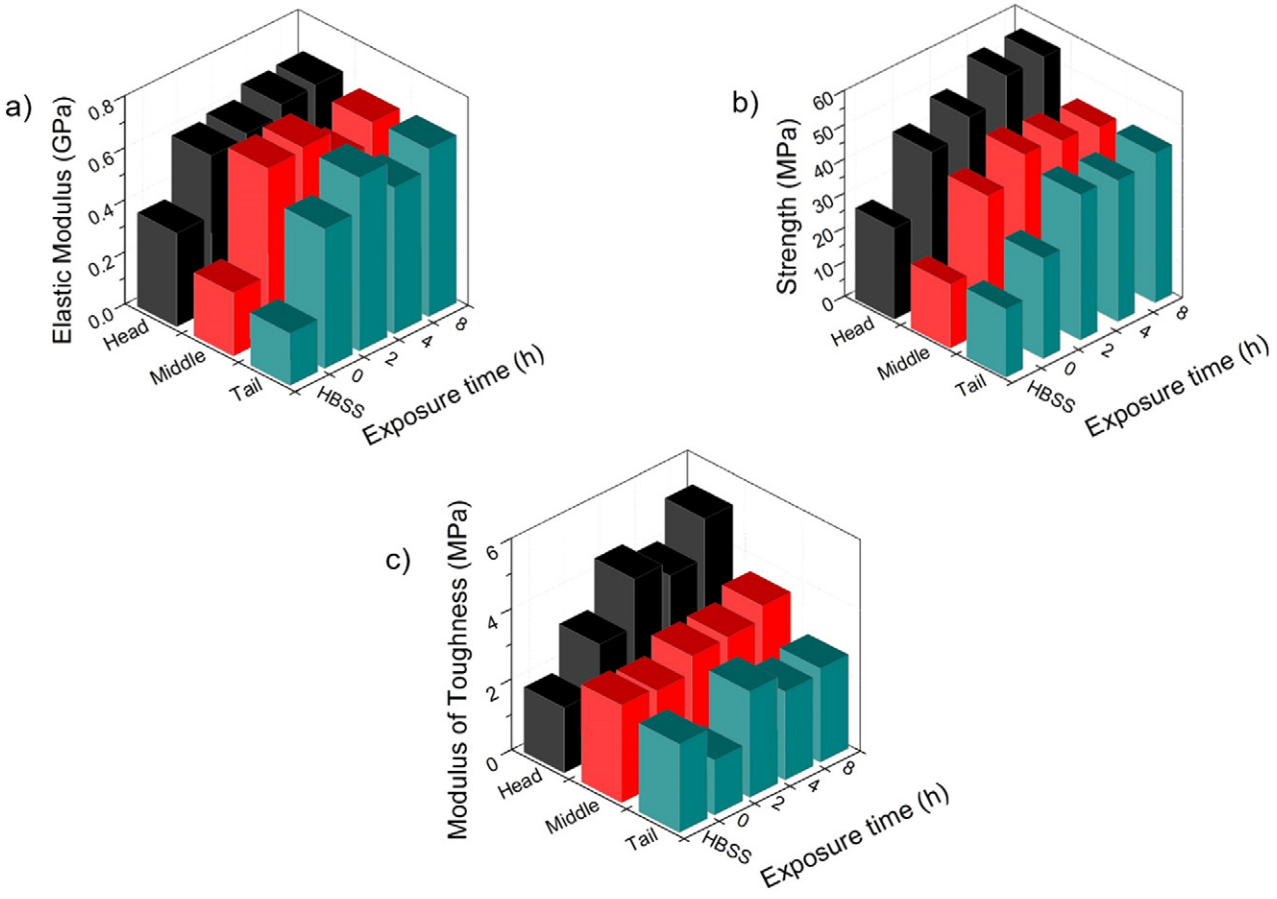

Fig. 4. Importance of ethanol exposure time on the mechanical behavior of the scales under uniaxial tension. a) Elastic modulus, b) strength, c) modulus of toughness.

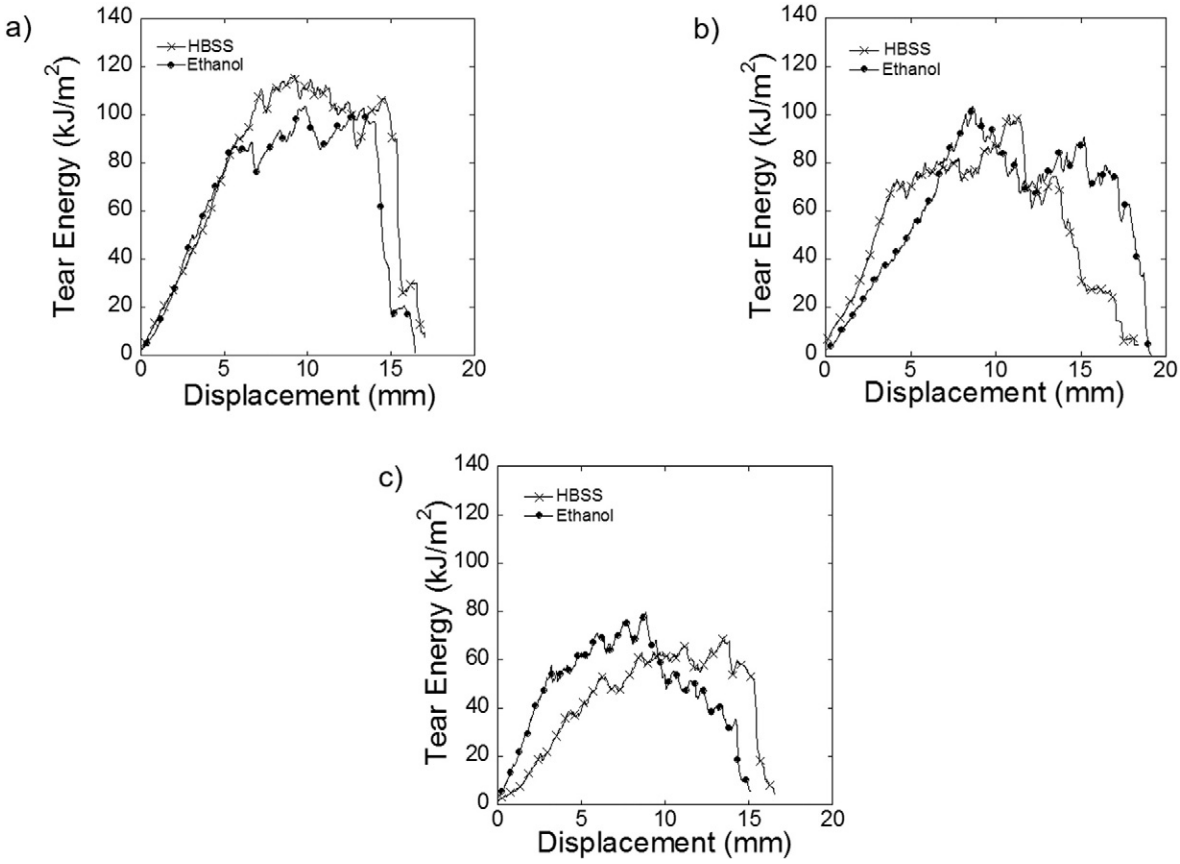

Fig. 5. Representative Tear energy vs. displacement responses from the tear tests performed on scales from the a) head, b) middle and c) tail regions. Results for the ethanol treatment correspond to immediate exposure (0 h).

treatment on the fracture resistance in Mode III loading was not consistent with that for tensile loading. For instance, for scales from the head there was a significant reduction ($p < 0.05$) in the tear energy and work to tear of with exposure to ethanol. In contrast, there was a significant increase ($p < 0.05$) in both the tear energy and work required to tear for scales from the middle region, whereas there was no significant difference ($p > 0.05$) in the tear resistance caused by exposure to ethanol for scales of the tail. When compared as a function of location, there is a reduction in the resistance to fracture of the scales from the head to the tail in the hydrated condition. Yet, the spatial distribution of the responses changes after exposure to ethanol. In terms of the tear energy, scales from the tail exhibited significantly lower values ($p \leq 0.05$) than the head and middle regions. But when evaluated in terms of the work, there was no significance difference ($p > 0.05$) in the tear resistance between the scales of the head and tail regions after ethanol exposure. Scales from the middle region exhibited the greatest tear resistance overall.

Fig. 7 shows the elemental composition of the scales in the three regions of evaluation. The composition was evaluated at nine discrete locations as described in Fig. 7(a), with one point located in the limiting layer and the remainder distributed over the remaining thickness of the elasmodine as a function of normalized distance. Results of the EDS analysis showed that the four main elements detected were Phosphorus, Calcium, Oxygen and Carbon. The mineral portion of the scales

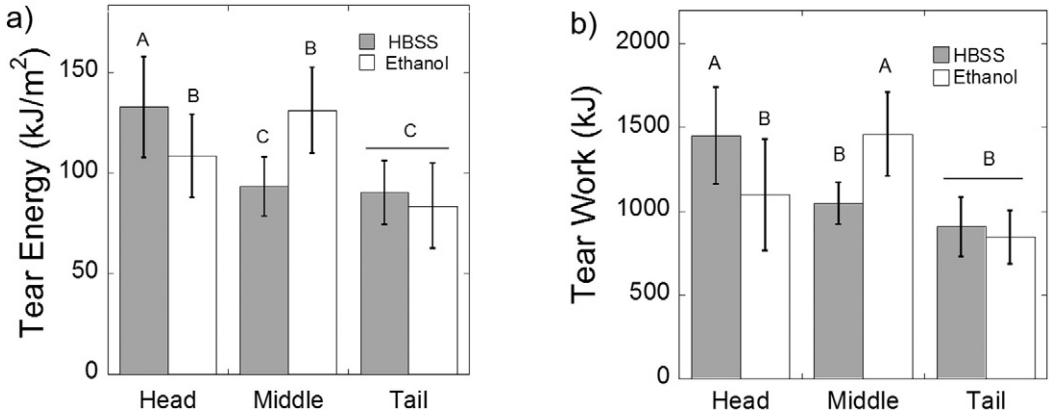

Fig. 6. Importance of ethanol exposure on the resistance to fracture of the scales under Mode III tear loading. a) Energy to failure, b) work to failure. Columns with different letters are significantly different ($p \leq 0.05$).

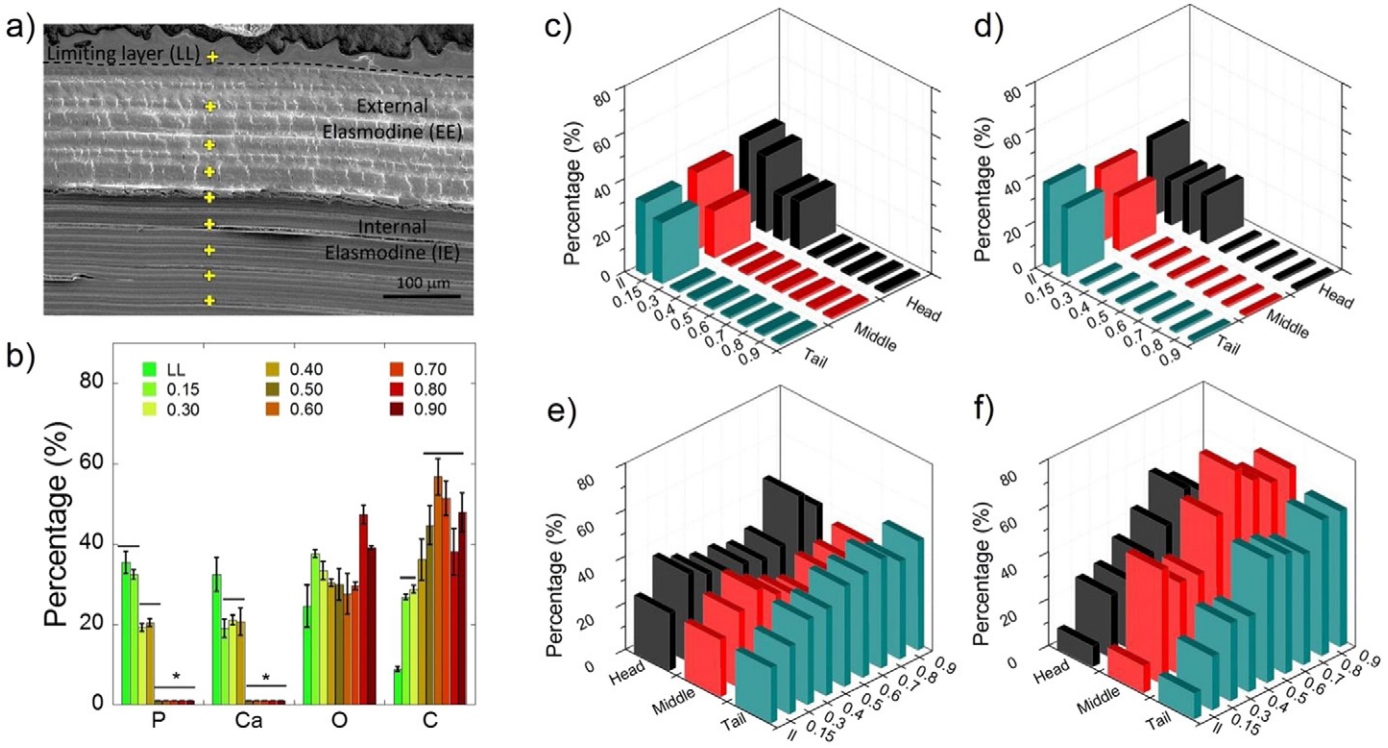

Fig. 7. Evaluation of the elemental composition of the scales and the differences with location. a) Micrograph from a head scale distinguishing the limiting layer (LL), as well as the internal (IE) and external elasmodine (EE). The series of points across the scale thickness represent the approximate locations for EDS analysis. The measurement depth from the LL was normalized with respect to the combined thickness of the external and internal elasmodine layers. b) Distribution of elements over the thickness of the head scales. Columns with different bar are significantly different. A comparison of the elemental distributions for the three regions of evaluation (head, middle and tail) is shown in (c)–(f). Elemental distributions for c) Phosphorus, d) Calcium, e) Oxygen, and f) Carbon are shown across the scale thickness. Note that there is no Phosphorus or Calcium in the internal elasmodine and the bars are shown for completeness across the thickness.

consisted of calcium deficient hydroxyapatite, as reported previously [6,13]. The relative presence and distribution of the major elements over the thickness of scales from the head region are shown in Fig. 7b. The Phosphorus and Calcium content was the greatest within the limiting layer and decreased with distance from this layer within the elasmodine. A comparison of the elemental composition for scales from the three regions of evaluation is presented in Fig. 7c–f. Clearly the presence of Phosphorus (Fig. 7c) and Calcium (Fig. 7d) is limited to the region adjacent to the limiting layer, especially in scales from the middle and tail regions.

4. Discussion

Previous studies concerning the structural behavior of fish scales have identified that the mechanical properties are dependent on the level of hydration and that a reduction in water content results in an increase in stiffness, strength and toughness [6,12,13]. Also relevant to the behavior of elasmoid scales, Garrano et al. [6] noted that the properties of scales from *C. carpio* are dependent on the anatomical position. When fully hydrated, scales from the head exhibited a strength and toughness nearly twice the values of those properties for the tail, whereas after dehydration in air there were limited differences in the mechanical properties of scales obtained from over the entire length of the fish. Those findings are not consistent with the distribution of properties resulting from chemical dehydration by ethanol treatment in Fig. 4. While the elastic modulus of scales from all three regions increased to the same maximum value, both the strength and MOT continued to exhibit differences with location after ethanol treatment. The effects of ethanol on the mechanical behavior and importance of spatial variations in microstructure on the observed responses require further discussion.

One of the primary contributions to the changes in properties with ethanol treatment is the development of interpeptide hydrogen bonds about the tropocollagen molecules. Water forms both intra- and interchain hydrogen bond bridges about the collagen molecules and peptides [26,27]. When the water is displaced by ethanol (a weaker hydrogen-bond-forming solvent), it allows direct hydrogen-bonding between the peptide chains. That results in a greater number of interpeptide hydrogen bonds at the molecular level, which in turn promotes stiffening at the macroscopic level. Gautieri et al. [17] reported that the unique mechanical properties of collagen microfibrils originate from their hierarchical structure at the nanoscale, and the cross-linking between the tropocollagen molecules. Though hydrogen bonds are rather weak due to their lower energy in comparison to the covalent bonds, an adequate volume fraction of interpeptide bonds enabled by removal of water can elicit substantial changes to the mechanical behavior of single fibrils [28], and dense fibril systems [26,27,29].

The effectiveness of polar solvents to form hydrogen bonds in collagen is often described in terms of the Hansen solubility parameter for hydrogen bonding (δ_h). Polar solvents with high δ_h values preferentially form hydrogen bonds with collagen peptides, thereby preventing the molecules from developing interpeptide bonds. Water has one of the highest reported δ_h values for polar solvents 37.3 $(J/cm^3)^{1/2}$. In the absence of water, or when the matrix is immersed in solvents with δ_h below 19 $(J/cm^3)^{1/2}$, which is the value postulated for collagen in air [26], interpeptide hydrogen bonding occurs. Thus, exposure of the scales to ethanol with δ_h of 19 $(J/cm^3)^{1/2}$ is expected to cause an increase in the stiffness and strength of the scales due to the displacement of water molecules and development of interpeptide hydrogen bonds. This mechanistic description is supported by the experimental results. Previous studies conducted with demineralized dentin have demonstrated this behavior as well and the importance of the solvent's δ_h [26,29,30]. Maciel et al. [29] showed that chemical dehydration by polar solvents is a time dependent process and that the removal of water requires time. Indeed, there were instantaneous changes in the

mechanical behavior of the scales, but they continued over time with diffusion of the miscible solvent (Fig. 3).

It is helpful to consider the changes in mechanical behavior resulting from ethanol exposure with regards to the hydrated condition. Fig. 8 shows the relative change in uniaxial properties with chemical dehydration after being normalized by the responses in HBSS. In Fig. 8a, the increase in elastic modulus of scales from the tail exceeds a factor of three, which is the largest of all changes documented. The elastic modulus of scales from the remaining two regions also increased with ethanol treatment, but to a lesser extent. After roughly 8 h in ethanol the elastic modulus reached an equivalent plateau in the three regions (Fig. 4a), which is consistent with dehydration in air [6]. The air-dried [6] and ethanol-treated carp scales exhibit similar values of elastic modulus (0.4–0.8 GPa), which may be expected due to the consistency in the Hansen solubility parameters for ethanol- and air-dried collagen.

What could cause the spatial variations in the degree of changes in elastic modulus with ethanol treatment? The difference in "stiffening" between the head, middle and tail regions is expected to arise from the spatial distribution in mineral (Fig. 7) and its interference with the hydrogen bonding. For instance, Pashley et al., [26] reported an increase in stiffness of fully demineralized and hydrated dentin of over 12 times when exposed to acetone. In the hydrated condition, the stiffness of scales is primarily dependent on the number of highly mineralized plies of the external elasmodine, which decreases from head to tail [7]. The mineral has been described as partially "shielding" the collagen in the hydrated tissues, and a reduction of load accommodated by the collagen [31]. The higher mineral content of scales from the head region (Fig. 7) resulted in larger stiffness in the hydrated condition (based simply on the rule of mixtures), but also limited the extent of additional hydrogen bonding during ethanol treatment. Increasing mineralization displaces water from collagen and the mineral crystals are also sites for water to bind [27]. Here we believe that the mineral interfered with the process of interpeptide hydrogen bonding in the presence of ethanol, which decreased the degree of stiffening overall.

Fig. 8b shows the normalized changes in strength with ethanol treatment. There was a uniform increase in strength of approximately a factor of two with respect to the hydrated condition for all three regions. Due to the uniformity in strengthening across the body of the fish, the head scales exhibited significantly larger strength ($p \leq 0.05$) than the other two regions after completion of the chemical dehydration. The increases in strength are lower than those for the modulus, which agrees with the results for chemical dehydration of demineralized [26] and fully mineralized [31] dentin. Surprisingly, the increase in strength of the scales is nearly equal to that reported for dentin. Furthermore, chemical dehydration by ethanol was more effective at promoting an increase in strength than dehydration in air [6]. As the effectiveness of air-drying is a function of the ambient humidity, the larger increase in strength by ethanol treatment is expected and results from the larger volume fraction of hydrogen bonds achieved by the polar solvent.

The distribution of normalized modulus of toughness after ethanol treatment is shown in Fig. 8c. Consistent with the changes in strength with dehydration, the largest increase in the MOT was approximately a factor of two. However, in contrast to the other properties, the maximum increase in toughness occurred to scales from the head region and not the middle or tail. We expect that this difference in behavior of the MOT is attributed to its dependence on sliding of the collagen molecules. Replacement of the water with weak hydrogen-bonding polar solvents not only promotes interpeptide bonding, but may also

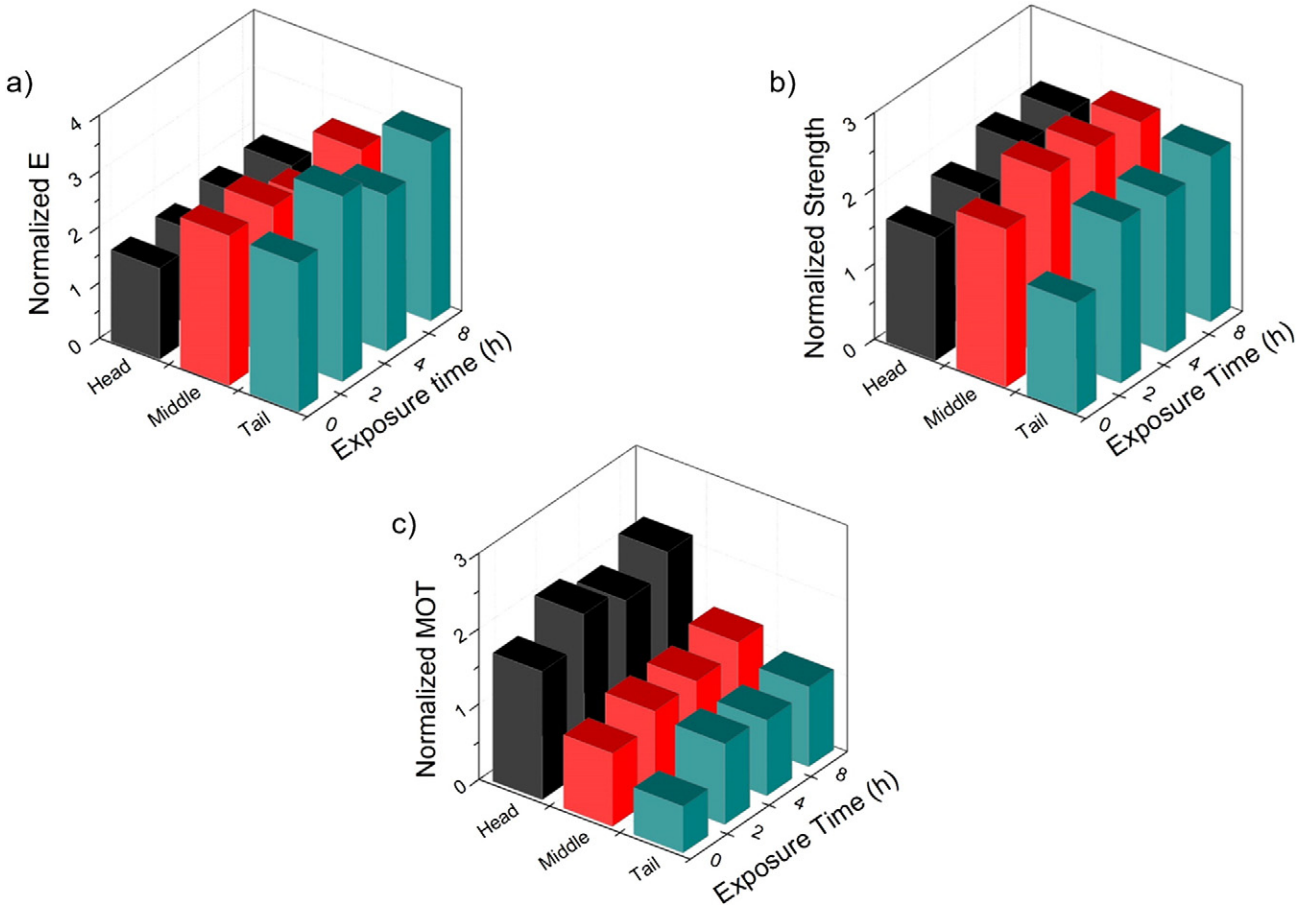

Fig. 8. Normalized mechanical behavior of the fish scales under uniaxial tension after exposure to ethanol with respect to the hydrated state: a) elastic modulus, b) strength, c) modulus of toughness.

change the structure of the collagen [30,31]. This disruption in molecular structure would undoubtedly interfere with the sliding of fibrils and potentially improve the effectiveness of the mineral platelets in providing resistance to inelastic deformation.

One interesting finding is that chemical dehydration of the scales with ethanol resulted in a higher modulus of toughness than dehydration in air [6]. Scales of the head exhibited a modulus of toughness of 3.5 MPa after 24 h in air, which is substantially lower than the maximum obtained for ethanol treatment of the head scales in Fig. 4c (5.5 MPa). Besides the influence of humidity in air-drying, there are two additional contributing factors. Both forms of dehydration (air and polar solvents) enable the development of interpeptide hydrogen bonds, which increase the resistance to sliding of the molecules. However, the ethanol also serves as a molecular lubricant and facilitates the rapid redevelopment of new hydrogen bonds with the nearest interpeptide neighbors without fracture. Free convection is not as efficient at removing the unbound water (related to ambient humidity), and does not result in removal of bound water. In contrast, polar solvents are able to remove free and even some bound water [28]. Nyman et al. [27] noted that the modulus of elasticity and strength of cortical bone was inversely correlated with the degree of bound water, whereas the toughness of bone was inversely correlated with free (mobile) water. Bone possesses a much higher mineral content than fish scales, and the differences in water content were associated with difference in age not dehydration by ethanol treatment. Hence, bone may not serve as an appropriate model for fish scale collagen. Nevertheless, it is clear that the presence of a fluid layer is essential to the toughness of collagen-based materials due to its contribution to plasticization of the fibrils [18,29,31].

In a recent study on the importance of temperature to the fracture resistance of carp scales under Mode III loading, the largest energy to fracture overall was exhibited by scales of the head region [7]. The resistance to fracture was found to correlate with the thickness of the external elasmodine and the number of highly mineralized plies of this region [7]. The resistance to fracture decreased with temperature and was speculated to result from the lower compliance of the scales, which prevented realignment of the fibrils to the direction of principal stress. Nalla et al. [18,31] found that chemical dehydration of dentin using polar solvents caused a significant increase in the fracture resistance of dentin under Mode I loading. The fracture toughness nearly doubled after submersion in alcohol with respect to the response in the fully hydrated condition (HBSS) and the process was also shown to be reversible with rehydration of the tissue. In those studies the rise in fracture toughness resulted from an increased potency of the extrinsic mechanism of toughening, which largely occurs as a result of the unbroken posterior bridging ligaments operating behind the crack tip. Although chemical hydration increased the stiffness and strength of the more highly mineralized scales of the head, the resistance to fracture decreased.

The fracture resistance of tissues under Mode III loading (i.e. the tear resistance) is rather seldom studied in comparison to Mode I. It does represent a very relevant mode of performance, especially in the assessment of very compliant systems. In Mode I, the direction of principal stress is coincident with one of the principal ply orientations. However, in Mode III the direction of principal stress is out of plane of all the plies and requires substantial reorientation of the collagen fibrils to align with the direction of maximum tensile stress. Yang et al. [1] recently evaluated the tear resistance of skin in tension and observed that it is nearly impossible to tear notched samples. They found that the remarkable tear resistance is attributed to straightening of the fibrils and reorientation to the tensile direction, elastic stretching and interfibrillar sliding. Reorganization and sliding of the fibrils are responsible for a redistribution of stress that causes notch blunting. Here is where we may understand the rather unexpected tear response of the head scales after ethanol treatment. If the tear resistance is dependent on fibril reorientation, it is perceivable that the combination of interpeptide bonding and larger mineral content inhibited this process. Indeed, the significant reduction in tear resistance of scales with reduction in temperature is at least partly due to the reduced mobility of fibrils and inability to undergo reorientation [7]. There was no significant difference in the tear resistance of scales from the tail in the HBSS and ethanol environments. Due to the low mineral content (Fig. 7b, c) of scales from this region, fibril reorientation should have been encumbered the least. It is plausible that intermolecular hydrogen bonding is less effective under large deformation due to the reduction in volume fraction of interpeptide bonds, and additional mechanisms of reinforcement become essential. Though speculative, that appears to be responsible for the significantly greater fracture resistance after ethanol treatment of scales from the middle region.

Results from this investigation have provided additional understanding regarding the effects from removal of water and molecular bonding to the mechanical behavior of fish scales. New findings were obtained regarding the relative importance of mineral content and molecular bonding to stiffness, strength and fracture resistance. Nevertheless, there are recognized limitations to the investigation that are important to consider. Ethanol was chosen for chemical hydration of the scales according to its application in other studies. Ethanol also has similar δ_h to that for collagen in air and provided an effective basis for examining the importance a fluid layer in chemical dehydration. Future work performed using polar solvents with $\delta_h < 19$ $(J/cm^3)^{1/2}$ could provide additional understanding. In addition, the degree of bound water removed from the collagen was not measured, which prevents the development of a complete understanding concerning the mechanisms responsible for the changes in properties. There are techniques for measuring the bound water content in tissues [32,33], and correlations have been established between this water and the mechanical properties of bone [27].

In bone, there are many layers of loosely and tightly bound water [34]. At the molecular scale, bound water molecules are trapped within and between the chains of the tropocollagen molecules, as well as within the apatite mineral structure (regarded as “structural water”). Water located in these individual compartments requires different levels of energy for removal. Far less is known regarding the layers of bound water in fish scale collagen. Thus, the difficulty of displacing the water in fish scales using polar solvents and the amount of remaining bound water after ethanol treatment are unknown. Future studies aimed at understanding the contributions of the bound water layers and mechanical behavior of fish scales may be fruitful, especially if the removal can be used to tune the mechanical behavior according to desired performance.

5. Conclusions

Elasmoid scales of the *C. carpio* were subjected to chemical dehydration by exposure to ethanol. The mechanical behavior of the scales was evaluated before and after ethanol treatment in uniaxial tension and via Mode III loading to fracture. Ethanol treatment caused an immediate increase in all components of the tensile response and additional secondary changes that reached stability after approximately two hours of exposure. Although the maximum elastic modulus, strength and toughness were exhibited by scales of the head region, the largest increase in these properties with ethanol treatment occurred to scales of the tail; the change was inversely proportional to the mineral content. There were significant and region-dependent changes in the fracture resistance of the scales with ethanol treatment, but they did not correlate with the degree of mineralization. Results indicate that interpeptide hydrogen bonding is important to the mechanical behavior of collagen tissues and that the relative contribution to mechanical behavior is also a function of mineral content. The modulus of toughness was the only property that increased with interpeptide hydrogen bonding and an increasing degree of mineralization.

Acknowledgments

This research was supported in part by seed grants from the University of Washington, Colciencias by contract 0210-2013, the Natural Science Foundation of Anhui Educational Commission (no. KJ2014A017), and the Ministry of education scientific research foundation for Returned Overseas Students (no. 2015KJS010003) and OEIAM (no. 201409).

References

[1] W. Yang, V.R. Sherman, B. Gludovatz, M. Mackey, E.A. Zimmermann, E.H. Chang, M.A. Meyers, Protective role of *Arapaima gigas* fish scales: structure and mechanical behavior, Acta Biomater. 10 (2014) 3599–3614.
[2] E.A. Zimmermann, B. Gludovatz, E. Schaible, N.K. Dave, W. Yang, M.A. Meyers, R.O. Ritchie, Mechanical adaptability of the Bouligand-type structure in natural dermal armour, Nat. Commun. 4 (2013) 2634.
[3] W. Yang, B. Gludovatz, E.A. Zimmermann, H.A. Bale, R.O. Ritchie, M.A. Meyers, Structure and fracture resistance of alligator gar (*Atractosteus spatula*) armored fish scales, Acta Biomater. 9 (2013) 5876–5889.
[4] W. Yang, I.H. Chen, B. Gludovatz, E.A. Zimmermann, R.O. Ritchie, M.A. Meyers, Natural flexible dermal armor, Adv. Mater. 25 (2013) 31–48.
[5] I.H. Chen, W. Yang, M.A. Meyers, Alligator osteoderms: mechanical behavior and hierarchical structure, Mater. Sci. Eng. C 35 (2014) 441–448.
[6] A.M.C. Garrano, G. La Rosa, D. Zhang, L.N. Niu, F.R. Tay, H. Majd, D. Arola, On the mechanical behavior of scales from *Cyprinus carpio*, J. Mech. Behav. Biomed. Mater. 7 (2012) 17–29.
[7] S. Murcia, M. McConville, G. Li, A. Ossa, D. Arola, Temperature effects on the fracture resistance of scales from *Cyprinus carpio*, Acta Biomater. 14 (2015) 154–163.
[8] R.K. Chintapalli, M. Mirkhalaf, A.K. Dastjerdi, F. Barthelat, Fabrication, testing and modeling of a new flexible armor inspired from natural fish scales and osteoderms, Bioinspir. Biomim. 9 (2014) 036005.
[9] B.J. Bruet, J. Song, M.C. Boyce, C. Ortiz, Materials design principles of ancient fish armour, Nat. Mater. 7 (2008) 748–756.
[10] A.K. Dastjerdi, F. Barthelat, Teleost fish scales amongst the toughest collagenous materials, J. Mech. Behav. Biomed. Mater. (2014) http://dx.doi.org/10.1016/j.jmbbm.2014.09.025.
[11] D. Zhu, C.F. Ortega, R. Motamedi, L. Szewciw, F. Vernerey, F. Barthelat, Structure and mechanical performance of a "modern" fish scale, Adv. Eng. Mater. 14 (2012) B185–B194.
[12] T. Ikoma, H. Kobayashi, J. Tanaka, D. Walsh, S. Mann, Microstructure, mechanical, and biomimetic properties of fish scales from *Pagrus major*, J. Struct. Biol. 142 (2003) 327–333.
[13] Y.S. Lin, C.T. Wei, E.A. Olevsky, M.A. Meyers, Mechanical properties and the laminate structure of *Arapaima gigas* scales, J. Mech. Behav. Biomed. Mater. 4 (2011) 1145–1156.
[14] F.G. Torres, O.P. Troncoso, J. Nakamatsu, C.J. Grande, C.M. Gomez, Characterization of the nanocomposite laminate structure occurring in fish scales from *Arapaima gigas*, Mater. Sci. Eng. C 28 (2008) 1276–1283.
[15] F.G. Torres, O.P. Troncoso, E. Amaya, The effect of water on the thermal transitions of fish scales from *Arapaima gigas*, Mater. Sci. Eng. C 32 (2012) 2212–2214.
[16] P.Y. Chen, J. Schirer, A. Simpson, R. Nay, Y.S. Lin, W. Yang, M.A. Meyers, Predation versus protection: fish teeth and scales evaluated by nanoindentation, J. Mater. Res. 27 (2012) 100–112.
[17] A. Gautieri, S. Vesentini, A. Redaelli, M.J. Buehler, Hierarchical structure and nanomechanics of collagen microfibrils from the atomistic scale up, Nano Lett. 11 (2011) 757–766.
[18] R.K. Nalla, J.H. Kinney, A.P. Tomsia, R.O. Ritchie, Role of alcohol in the fracture resistance of teeth, J. Dent. Res. 85 (2006) 1022–1026.
[19] E. Osorio, M. Toledano, F.S. Aguilera, F.R. Tay, R. Osorio, Ethanol wet-bonding technique sensitivity assessed by AFM, J. Dent. Res. 89 (2010) 1264–1269.
[20] J. Kim, L. Gu, L. Breschi, L. Tjäderhane, K.K. Choi, D.H. Pashley, F.R. Tay, Implication of ethanol wet-bonding in hybrid layer remineralization, J. Dent. Res. 89 (2010) 575–580.
[21] D. Zhang, A. Nazari, M. Soappman, D. Bajaj, D. Arola, Methods for examining the fatigue and fracture behavior of hard tissues, Exp. Mech. 47 (2007) 325–336.
[22] D. Zhu, L. Szewciw, F. Vernerey, F. Barthelat, Puncture resistance of the scaled skin from striped bass: collective mechanisms and inspiration for new flexible armor designs, J. Mech. Behav. Biomed. Mater. 24 (2013) 30–40.
[23] D. Zhang, D. Arola, Applications of digital image correlation to biological tissues, J. Biomed. Opt. 9 (2004) 691–699.
[24] D. Zhang, M. Luo, D. Arola, Displacement/strain measurements using an optical microscope and digital image correlation, Opt. Eng. 45 (2006) (033605-033605).
[25] ASTM, Tear-Propagation Resistance (Trouser Tear) of Plastic Film and Thin Sheeting by a Single-Tear Method, in D-1938, 2008.
[26] D.H. Pashley, K.A. Agee, R.M. Carvalho, K.W. Lee, F.R. Tay, T.E. Callison, Effects of water and water-free polar solvents on the tensile properties of demineralized dentin, Dent. Mater. 19 (2003) 347–352.
[27] J.S. Nyman, Q. Ni, D.P. Nicolella, X. Wang, Measurements of mobile and bound water by nuclear magnetic resonance correlate with mechanical properties of bone, Bone 42 (2008) 193–199.
[28] C.A. Grant, D.J. Brockwell, S.E. Radford, N.H. Thomson, Tuning the elastic modulus of hydrated collagen fibrils, Biophys. J. 97 (2009) 2985–2992.
[29] K.T. Maciel, R.M. Carvalho, R.D. Ringle, C.D. Preston, C.M. Russell, D.H. Pashley, The effects of acetone, ethanol, HEMA, and air on the stiffness of human decalcified dentin matrix, J. Dent. Res. 75 (1996) 1851–1858.
[30] D.H. Pashley, K.A. Agee, M. Nakajima, F.R. Tay, R.M. Carvalho, F.J. Harmon, F.A. Rueggeberg, Solvent-induced dimensional changes in EDTA-demineralized dentin matrix, J. Biomed. Mater. Res. 56 (2001) 273–281.
[31] R.K. Nalla, M. Balooch, J.W. Ager, J.J. Kruzic, J.H. Kinney, R.O. Ritchie, Effects of polar solvents on the fracture resistance of dentin: role of water hydration, Acta Biomater. 1 (2005) 31–43.
[32] W. Robinson, Free and bound water determinations by the heat of fusion of ice method, J. Biol. Chem. 92 (1931) 699–709.
[33] F.W. Wehrli, M.A. Fernández-Seara, Nuclear magnetic resonance studies of bone water, Ann. Biomed. Eng. 33 (2005) 79–86.
[34] M. Granke, M.D. Does, J.S. Nyman, The role of water compartments in the material properties of cortical bone, Calcif. Tissue Int. 97 (2015) 292–307.